LABORATORI NAZIONALI DI FRASCATI
SIS – Pubblicazioni

LNF–96/038 (P)
29 Luglio 1996

Quasi-real Compton Scattering at DAΦNE for a Continuous Calibration of the KLOE Detector

A. Courau
Laboratoire de l'Accélérateur Linéaire,
IN2P3-CNRS et Université de Paris-Sud, F-91405 Orsay Cedex, France
and
G.Pancheri
INFN, Laboratori Nazionali di Frascati,
P.O. Box 13, I00044 Frascati, Italy

Abstract

Quasi-real Compton scattering, previously used in e^+ e^- and e p collisions for luminosity measurements and detector calibration at PEP and HERA, is discussed for the energy range available at the construenda ϕ-factory DAΦNE. We show that the very high rate expected at DAΦNE makes this process particularly convenient for a continuous calibration of the KLOE detector over the full angular range, directly from the data.

The use of overconstrainted quasi-real Compton $e\gamma$ events at e^+e^- [1] and ep colliders[2] was suggested in 1985 as means to perform luminosity measurement, search for excited electrons and detector calibration. This method was indeed successfully used for e^*-searches at PEP [3], PETRA[4], Tristan [5], LEP1 [6] and at HERA [7], as well as for calibration and luminosity measurements at PEP and at HERA [8]. In this note, we apply it to the calibration of the detector KLOE [9], which will study CP violation in the kaon system at the ϕ-factory DAΦNE , under completion at Frascati. The KLOE detector covers a large angular range, i.e. 98% of the full solid angle, and the calibration of the electromagnetic calorimeter is presently assigned to a momentum measurement in the high precision tracking chamber. Our suggestion is for an additional calibration method, to be used independently (from the performance) of the tracking chamber. The very high rates expected through quasi-real Compton scattering described below should also allow for a control of the efficiency of the tracker and its rate of photon conversion, as well as a precise measurement of the position of the detector relative to the beam.

Like "Bremsstrahlung" and "radiative Bhabha scattering at finite angle", the Compton process considered here is just a specific configuration of the reaction $ee \to ee\gamma$, shown in Fig.1. Looking at both the diagrams with a photon

PACS N.: 13.40.Ks

Submitted to Physics Letters

exchange which contribute to this reaction [1], one notices that the corresponding amplitude contains two propagators $\frac{dq^2}{q^2}\frac{dq'^2}{q'^2-m_e^2}$ (resp. $\frac{dq^2}{q^2}\frac{dq''^2}{q''^2-m_e^2}$). Clearly then, the dominant contribution to the cross-section stems from con-

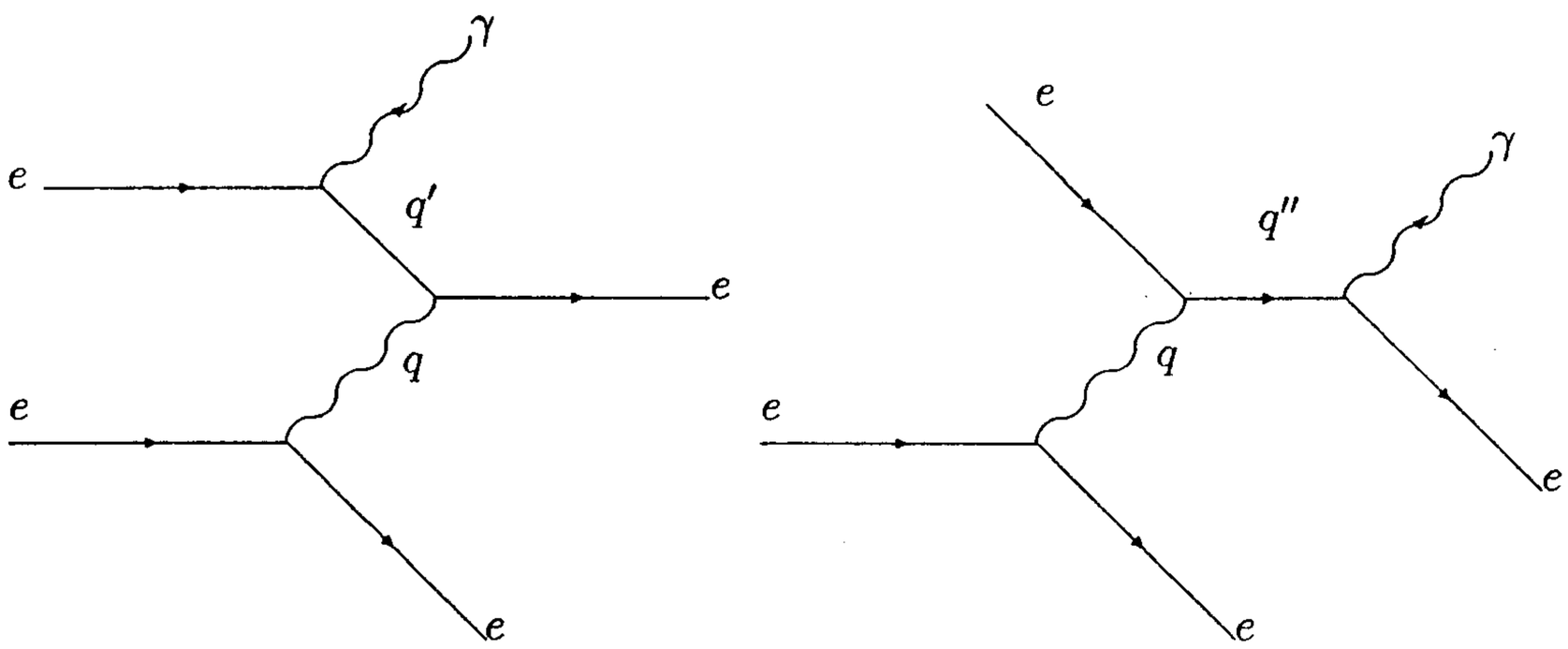

Figure 1: Feynman diagrams of $ee \to ee\gamma$ with photon exchange

figurations where both $q^2, q'^2(q''^2)$ stay close to zero with the electrons and the photon going practically straightforward (undetected by the central detector). This configuration is the main contribution to the so-called "Bremsstrahlung" (or "small angle radiative Bhabha") and it leads to a cross-section so large that it could prevent the use of any tagging system at zero degree. Computation of the rate expected at DAΦNE for the designed nominal luminosity, $5 \times 10^{32}\ cm^{-2}\ sec^{-1}$, was performed analytically using a no-recoil approximation [10] and through a Monte-Carlo by M. Greco and collaborators[11]. Both studies conclude that the rate of electrons which have lost an energy larger than 70 MeV will be of the order of 30 MhZ ($\sim$0.1 event per bunch crossing)

When one of the two q^2 is not close to zero, particles, deflected at a finite angle, will be observed in the central detector . In this case, the cross-section will be dominated by the other q^2 being close to zero, and two different kinematical configurations giving rise to still relatively significant counting rates, will be observed:

1. $q'^2(q''^2) \to 0$ with $|q^2| >> |q'^2|, (|q''^2|)$, corresponding to the so called "Radiative Bhabha scattering at finite angle" with both electrons detected at finite angle and the radiated photon emitted along the incident (outgoing) electron.

2. $q^2 \to 0$ with $|q'^2|(|q''^2|) >> |q^2|$ which is what we call "Quasi-real Compton" with an electron and a photon detected in the central region, the other electron being scattered at zero degree.

It is the second of these configurations which we shall consider here. The principal characteristics of quasi-real Compton scattering is the overconstrained

[1] Note that $e^+e^- \to e^+e^-\gamma$ also implies additional annihilation grahs.

kinematics which defines the energy of the photon and of the observed electron through the simultaneous measurement of their scattering angle in the Laboratory frame. Thus an angular measurement from the data itself can lead to energy calibration. To illustrate the method, we shall first sketch the relevant kinematics and cross-section formulae. Then a discussion of the results shall follow.

For simplicity, we shall neglect here the beam-crossing angle of DAΦNE (this can be easily introduced through a Monte Carlo) and shall consider the e^+e^- system to be the Laboratory system for which we employ the following notation:

$\vec{p_e}$ and E_0 are the momentum and energy of the incident electron, E_γ the energy of the quasi-real photon and $\sqrt{s} = 2E_0$ the total incident energy;

$E'_{e,\gamma}, \Theta_{e,\gamma}, \Phi_{e,\gamma}$ are respectively the energy, polar and azimutal angles of the outgoing electron and photon; $\Delta\varphi = \Phi_e - \Phi_\gamma$ is the acoplanarity angle between the electron and photon;

W,$\mid \Sigma\vec{p_t} \mid$, $\vec{\beta}$ and E_{vis} are the invariant mass, the transverse momentum, the velocity and the visible energy of the observed $e\gamma$ system.

As q^2 tends to zero, the electron "generating" the photon is scattered at an angle close to zero degree and remains unseen. One thus observes only one electron and the photon (i.e. (e^+,γ) or (e^-,γ)) with :

$$\mid \Sigma\vec{p_t} \mid \to 0,\ \Delta\varphi \to \pi,\quad \vec{\beta} \parallel \vec{p_e}$$

and the kinematics is overconstrained since one has:

$$E_\gamma = \frac{W^2}{4E_0} = E_{vis} - E_0 = E_0\frac{1-\mid\vec{\beta}\mid}{1+\mid\vec{\beta}\mid} \qquad \begin{cases} W^2 = & 4E_0E_\gamma & = 2E'_eE'_\gamma(1-\cos(\Theta_e+\Theta_\gamma)) \\ E_{vis} = & E_0+E_\gamma & = E'_e+E'_\gamma \\ \mid\vec{\beta}\mid = & \dfrac{E_0-E_\gamma}{E_0+E_\gamma} & = \dfrac{\sin(\Theta_e+\Theta_\gamma)}{\sin\Theta_e+\sin\Theta_\gamma} \end{cases}$$

Let us note that the charge of the observed electron $e^\pm$ is correlated to the observed acollinearity since $\vec{\beta}$ is obviously in the opposite direction of the incident quasi-real photon ($E_\gamma < E_0$) and that the visible energy is larger than the beam energy ($E_{vis} > E_0$)

These relations follow by considering this as a Compton scattering, in which a quasi-real photon generated by one beam undergoes a head-on collision with an electron from the other beam. Therefore there are only three independent parameters W/2, $\theta^\star$ and $\varphi^\star$ (energy, polar and azimuthal angles of the outgoing electron in the $e\gamma$ system), while there are 6 measured quantities $(E', \Theta, \Phi)_{e,\gamma}$. Setting[2],

$Y = 1/2\ln(s/W^2)$	the rapidity of the e-γ system in the Lab.
$y^\star = -\ln(\tan(\theta^\star/2))$	the rapidity of the outgoing e in the $e-\gamma$ system
$y_{e,\gamma} = -\ln(\tan(\Theta_{e,\gamma}/2))$	the rapidity of the outgoing e and γ in the Lab.

[2] Θ_e, Θ_γ are defined with respect to $\vec{\beta}$ which is determined from the acollinearity.

and using $y_{e,\gamma} = Y \pm y^\star$, $Y = (y_e + y_\gamma)/2$ and $y^\star = (y_e - y_\gamma)/2$, one also derives:

$$W^2/s = \tan(\Theta_e/2)\tan(\Theta_\gamma/2)$$

$$\tan\theta^\star = \tan(\Theta_e/2)/\tan(\Theta_\gamma/2)$$

$$\varphi^\star = \Phi_e \ (= \pi - \Phi_\gamma)$$

The full kinematics of such events can be then obtained from the measurement of the angles alone, which leads to 3 constraints over $\Delta\Phi$, E'_1, E'_2.

The result is that Compton events can be selected by looking at events with 2 and only 2 electromagnetic clusters (only one of which is associated with a track of well defined charge $e^\pm$), coplanar $\Delta\Phi = \pi$, and with $\mid \Sigma\vec{p_t} \mid \sim 0$ and $E_{vis} > E_0$, with remaining kinematical constraints

$$E'_e(\Theta_e, \Theta_\gamma) = \frac{2E_0 \sin\Theta_\gamma}{\sin\Theta_e + \sin\Theta_\gamma + \sin(\Theta_e + \Theta_\gamma)}$$

$$E'_\gamma(\Theta_e, \Theta_\gamma) = \frac{2E_0 \sin\Theta_e}{\sin\Theta_e + \sin\Theta_\gamma + \sin(\Theta_e + \Theta_\gamma)}$$

Therefore, the measurement of both angles can be used to perform the energy calibration of the electromagnetic calorimeter, to determine its experimental resolution and to test the linearity of the response according to the energy and to the nature of the particle (e or γ). Those relations can also be used to determine the relative position of the detector with respect to the beam.

Let us note that we do not need the identifications of the photon and the electron, the energy of each cluster being only defined by the two angles (replace index e, γ by index 1,2) and we do not necessarily need to use track information in the selection (i.e only one track and defined charge). Now looking at the observed tracks, it is also possible to check the value of the magnetic field and, from the comparison of events with respectively 0 track,1 track and 2 tracks, to determine the efficiency of the tracker and its rate of photon conversion. All these results can be obtained by (fitting only) the data itself. They include the experimental effects and do not need a priori any Monte Carlo simulation.

Such analyses were successfully performed for the H1 detector [8], and since, as shown below, the number of Compton events per second expected within KLOE at DAΦNE will be be of the same order of magnitude as the total number of events obtained in one year at H1, similar analysis should be likewise very relevant at DAΦNE.

Having established the event kinematics for $|q^2| \ll W^2$, let us now proceed to discuss the cross-sections. In general, for the process $ee \to ee\gamma$, through the helicity amplitudes one obtains [2]

$$\frac{d\sigma^{ee\to ee\gamma}}{dy\ dq^2 d\Omega^\star} = f^{\gamma^\star/e}(y, q^2)\frac{d\sigma^{\gamma^\star e\to\gamma e}}{d\Omega^\star}$$

with

$$f^{\gamma^*/e}(y,q^2) = \frac{\alpha}{\pi y}\left[(1-y+y^2/2) - (1-y)\frac{q^2_{min}}{q^2}\right]\frac{1}{q^2}$$

$$\frac{d\sigma^{\gamma^* e\to\gamma e}}{d\Omega^*} = \frac{d\sigma_T}{d\Omega^*} + \epsilon\frac{d\sigma_L}{d\Omega^*} - \sqrt{2\epsilon(1+\epsilon)}\frac{d\sigma_{TL}}{d\Omega^*}\cos\phi^* + \epsilon\frac{d\sigma_{TT}}{d\Omega^*}\cos 2\phi^*$$

and, with $Q^2 = -q^2$,

$$\frac{d\sigma_T}{d\Omega^*} = \frac{\alpha^2}{W^2+Q^2}\left[\frac{W^2}{(W^2+Q^2)(1+u^*+\eta)} + \frac{(W^2+Q^2)(1+u^*)}{4W^2} + \frac{Q^2(1-u^*)}{W^2(1+u^*+\eta)} + \frac{Q^2(1-u^*)}{2(W^2+Q^2)}\right.$$

$$\frac{d\sigma_L}{d\Omega^*} = \frac{\alpha^2}{W^2+Q^2}\left[\frac{Q^2(1-u^*)}{W^2+Q^2}\right]$$

$$\frac{d\sigma_{TL}}{d\Omega^*} = \frac{\alpha^2}{W^2+Q^2}\left[\frac{\sqrt{Q^2(1-u^{*2})}W}{2(W^2+Q^2)}\left[1+\frac{Q^2}{W^2}\frac{1-u^*}{1+u^*+\eta}\right]\right]$$

$$\frac{d\sigma_{TT}}{d\Omega^*} = \frac{\alpha^2}{W^2+Q^2}\left[\frac{Q^2(1-u^*)}{2(W^2+Q^2)}\right]$$

where $\quad y = \dfrac{W^2+Q^2}{s} \qquad \epsilon = \dfrac{1-y}{1-y+y^2/2} \qquad \eta = \dfrac{2m_e^2W^2}{(W^2+Q^2)^2}$

and $u^* = \cos\theta^*$, $d\Omega^* = d\cos\theta^* d\phi^*$ are defined in the center of mass of the $e\gamma$ system. Notice that, wherever it can be safely done, we neglect terms of order m_e^2.

For $Q^2 << W^2$, using the EPA, (i.e neglecting terms in Q^2/W^2 and integrating over the azimuthal angle) the cross-section becomes simply the convolution of

$$d^2N(X,q^2) = \frac{\alpha}{\pi}\left[(1-X+X^2/2) - (1-X)\frac{q^2_{min}}{q^2}\right]\frac{dX}{X}\frac{dq^2}{q^2}$$

with, for $u^* > -1$

$$d\sigma_{compton} = \frac{2\pi\alpha^2}{W^2}\left(\frac{1}{1+u^*} + \frac{1+u^*}{4}\right)du^*$$

where

$$X \equiv \frac{E_\gamma}{E_0} = \frac{W^2}{s} = \frac{E_{vis}-E_0}{E_0} = \frac{1-\beta}{1+\beta} = \tan\frac{\Theta_e}{2}\tan\frac{\Theta_\gamma}{2}$$

and

$$\cos\Theta_e = \frac{\beta-u^*}{1-\beta u^*}, \qquad \cos\Theta_\gamma = \frac{\beta+u^*}{1+\beta u^*}, \qquad \beta \equiv |\vec{\beta}|$$

Then an analytic Weiszäcker-Williams computation of the cross section, in an angular acceptance given in the Laboratory by $U^{e,\gamma}_{min} < \cos\Theta_{e,\gamma} < U^{e,\gamma}_{max}$, leads, in straightforward fashion, to a simple product of the equivalent photon spectrum integrated over q^2 with the Compton cross-section integrated over u^*, i.e., since $|q^2_{max}| >> |q^2_{min}|$, the product of

$$dN(W) = \frac{2\alpha}{\pi W}\left[\frac{s^2+(s-W^2)^2}{s^2}\ln\frac{Q_{Max}}{Q_{min}} - \frac{s-W^2}{s}\right]dW,$$

with

$$\sigma_{compton} = \frac{\pi\alpha^2}{2W^2}\left[(u_{max}-u_{min})(1+\frac{u_{max}+u_{min}}{2}) + 4\ln\frac{1+u_{max}}{1+u_{min}}\right]$$

$$\frac{Q_{max}}{Q_{min}} = Inf\left[\frac{\eta s}{m_e W}, \frac{E_0(s-W^2)}{m_e W^2}\right]$$

$$u_{min} = Sup\left[\frac{U^e_{min}-\beta}{1-\beta U^e_{min}}, \frac{\beta-U^\gamma_{max}}{1-\beta U^\gamma_{max}}\right]$$

$$u_{max} = Inf\left[\frac{U^e_{max}-\beta}{1-\beta U^e_{max}}, \frac{\beta-U^\gamma_{min}}{1-\beta U^\gamma_{min}}\right]$$

where $\eta < 1$ is an experimental cut ($\mid \Sigma\vec{p_t} \mid < \eta W$) within which the various approximations remain valid, $\beta = (s-W^2)/(s+W^2)$, and $U_{max,min}$ defines the angular acceptance in the Laboratory system. For symmetrical acceptance, $|cos\Theta_{e,\gamma}| < U_o$, the above expression is further simplied to

$$\sigma_{compton} = \frac{\pi\alpha^2}{W^2}\left[u_o + 2\ln\frac{1+u_o}{1-u_o}\right] \quad with \;\; u_o = \frac{U_o-\beta}{1-\beta U_o}$$

Let us note that:

- There is an additional factor two because either electron beam can interact with the photon generated by the other one
- The cross section can be equivalently expressed in terms of W, E_{vis} or β

$$d\sigma \propto \frac{dW}{W^3} \cong \frac{dE_{vis}}{(E_{vis}-E_0)^2} \cong \frac{(1+\beta)^2 d\beta}{(1-\beta)^4}$$

  However, when X,E_γ,W or E_{vis} increase, β decreases and the acceptance in the $e\gamma$ C-of-M increases. Therefore the integration over the acceptance slightly compensates the very strong W, β or E_{vis} dependence.

- For an angular acceptance given in the Lab by $\mid \cos\Theta_{e,\gamma} \mid < \cos\Theta_0$, the maximal and minimal value of $W^2 = s\tan(\Theta_\gamma/2)\tan(\Theta_e/2)$ are respectively given by s and $s\tan^2(\Theta_0/2)$ so that, for the overall cross-section, one has

$$\sigma \propto 2f(\Theta_0)(\ln\frac{E_0}{m_e})/s$$

This implies that for a given detector (with the same angular acceptance) the cross-section at DAΦNE is 6000 times larger than at LEP100, and, given the difference in expected luminosity, the rate of $e\gamma$ Compton events more than five orders of magnitude larger.

- At Hera, where the electron scatters with a photon generated by the proton beam, the cross-section loses the factor 2, relative to the e^+e^- case, and it is smaller because of the mass of the proton and its non point-like nature [2]. An exact and complete MonteCarlo exists [2] and it is used in H1 for luminosity measurement[6]. Assuming in first approximation, that the inelastic contribution compensates the effects of the electric and magnetic form factors in the elastic one (i.e. considering the proton as point-like), one gets

$$\sigma \propto f(\Theta_0)(\ln \frac{E_p}{M_p})/s$$

so that, for the same acceptance, $\sigma_{Hera}/\sigma_{DA\Phi NE}$ is of order 5×10^{-6}. Actually the acceptance of H1 goes down to smaller angles than the ones accepted at KLOE, but the larger luminosity expected at DAΦNE compensates for this difference and one can estimate that the number of events expected per second within KLOE (see below) would be of the same order as the number of events[3] accumulated by H1 in one year [8].

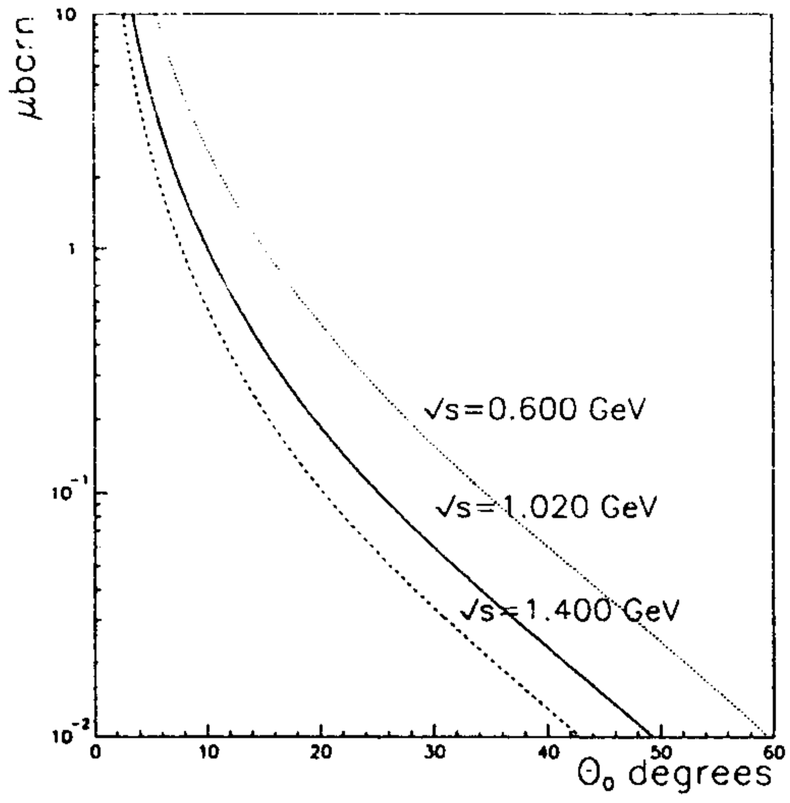

Fig. 2: Cross-section of quasi-real Compton at DAΦNE with respect to the angular acceptance of both the electron and photon given by $|\cos\Theta_{e,\gamma}| \leq \cos\Theta_0$

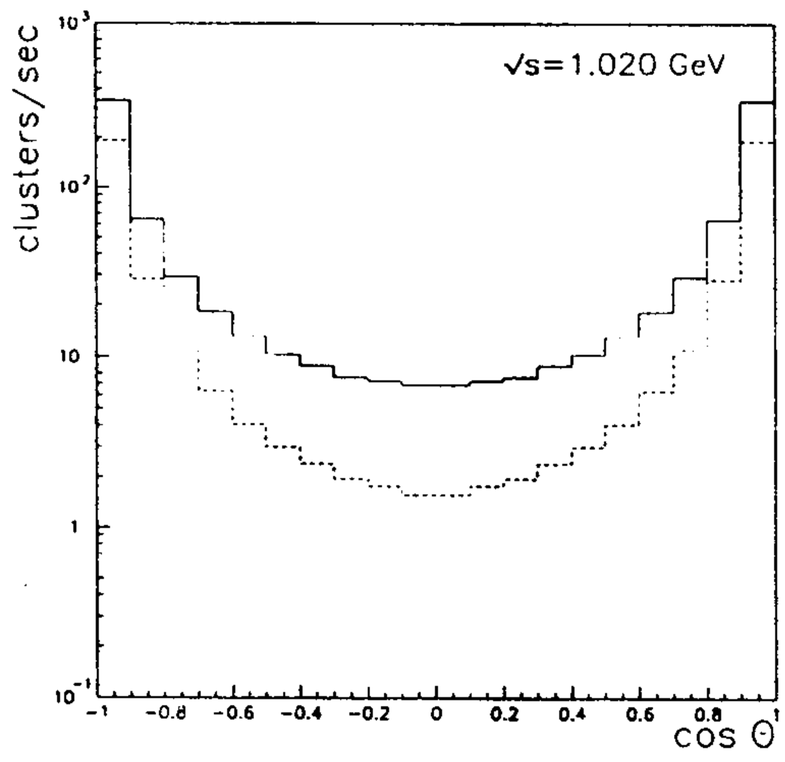

Fig. 3: Rate of clusters per second with respect to their emission angles for a luminosity of $5 \times 10^{32} cm^{-2} sec^{-1}$ and $|\cos\Theta_{e,\gamma}| \leq 0.985$. (Dashed histogram corresponds to photons)

We shall now discuss more in details some predictions for the DAΦNE case. The cross section expected for this process in the range of energies which will be

[3]At H1, the number of quasi-real Compton events analyzed, has been $\approx 250, 1500$ and 1000 in 1993, 1994 and 1995 respectively.

available at DAΦNE, is shown in Fig. 2 with respect to the angular acceptance of the detector. One notices that for KLOE, with $|\cos\Theta| \leq 0.985$, this cross-section is of the order of 1 μbarn and, for a luminosity of $5 \times 10^{32} cm^{-2} sec^{-1}$, this leads to a rate of 500 evts/sec (i.e.10^3 clusters/sec).

Obviously, the particles tend to be peaked at small angles. However, as shown in Fig. 3, the rate of clusters remains significant at any angle. Of course, the rate of one cluster at a given angle depends upon the minimal value of the acceptance of the other one (see Fig. 4). Nevertheless, the cross section and the rates for a cluster at large angle remain large when the second one is at small angle (see Fig. 4) and is still significant even for both particles emitted at relatively large angle (Fig. 2).

We have used analytic approximations in order to show the main characteristics. Clearly the beam crossing angle and the exact dynamics and kinematics can be included through a Monte Carlo calculation. Notice however, that for the calibration of the detector, one does not need a priori any Monte Carlo simulation. As far as the errors on the energy are concerned, they essentially arise from the experimental resolutions and not from the various approximations of the overdominant contribution of quasi-real photons (for example, at small $|\Sigma\vec{p_t}|$and acoplanarity $\Delta\varphi \sim \pi$, the theoretical error is negligible with respect to the experimental uncertainty). To show the precision of this method for energy calibration, we shall briefly outline the main steps involved in the analysis, reserving to a longer work the complete description.

The experimental resolution, ΔE, can be obtained by fitting the experimental distribution of the difference $E(\Theta_k, \Theta_j) - E_{i,measured}$ and the calibration factor K can be determined by minimizing

$$\chi^2 = \Sigma(E(\Theta_k, \Theta_j) - K E_{i,measured})^2/(\Delta E_i)^2$$

The precision for determining the calibration factor K, is obtained from the value of ΔK such that $\chi^2 = \chi^2_{min} + 1$, i.e.

$$(\Delta K)^{-2} = \sum_{N_{clus}} (\frac{E_i}{\Delta E_i})^2$$

ΔE is the convolution of the errors coming from the energy resolution in the calorimeter, ΔE_{cal}, and the angular resolution $\Delta E(\Theta_e, \Theta_\gamma) \equiv \Delta E_\Theta$. In practice, most of the error comes from the calorimeter. Examining for simplicity the particular case $\Theta_e = \Theta_\gamma = \Theta$, one has $E(\Theta_e, \Theta_\gamma) = E_0/(1 + \cos\Theta)$ and

$$\frac{\Delta E_\Theta}{E} = \frac{\sin\Theta}{1 + \cos\Theta}\Delta\Theta$$

In KLOE, the expected angular accuracy is better than 10^{-2}, giving an error ΔE_Θ an order of magnitude smaller than the one from the calorimeter resolution $\Delta E_{cal} = 0.05\sqrt{E(GeV)}$. For an average energy of each cluster around $E_{beam}/2 = 0.25 GeV$, this corresponds to $\Delta E/E \approx 0.1$, and thus to

$$< \frac{\Delta K}{K} > \approx \frac{0.1}{\sqrt{N}}$$

Comparison with HERA case[8], where $< \frac{\Delta E}{E} > \approx \frac{0.3}{\sqrt{15}}$ shows that the main difference is in the rates. Thus, at DAΦNE , in 10 seconds of data taking at the rate of 1000 *cluster/sec* (see Fig. 3), it should be possible to reach an accuracy better than 1 per mille.

Notice that the accuracy of the method is a priori limited by the presence of radiative corrections, to wit initial state radiation (ISR) from the colliding Compton electron (radiation from the final state plays no role, since the energy is measured in the calorimeter). ISR represents the most important effect [12] on the calibration method just discussed, as it affects not only the total cross section (which is reduced by 10% at DAΦNE with the cuts discussed below) but also the energy involved in the Compton process and thereby, the kinematical relations between energy and angles of the outgoing particles. As far as calibrations are concerned, we do not worry about absolute normalization and the 10% reduction of the cross-section does not intefere with the precision of the method we have discussed. Changes in the kinematics are more problematic and the full evaluation of these radiative corrections will then require a Monte Carlo with full detector simulation, which is under preparation. We shall here outline the main characteristics of these effects.

The contribution from ISR can be taken into account using the so-called peaking approximation. This procedure is justified by the fact that the radiated photon and the scattered one are emitted at different angles and thus can be distinguished, so that interference terms are suppressed. Actually we introduce an energy loss of the initial electron according to a probability law given the semi-classical formula [13]:

$$dP(k) = \beta\ k^{\beta-1}(1 - k + k^2/2)dk$$

with[4]

$$\beta = \frac{2\alpha}{\pi}(\ln\frac{2E_0}{m_e} - \frac{1}{2})$$

where k is the fraction of incident electron energy carried off by the radiated photon. Let us note that the hard-photon tail of the radiated spectrum has a low emission probability, but on the other hand it leads to smaller values of W, leading to an increase of the Compton cross section. However, it is possible to eliminate (to a large extent) the hard photon tail by imposing a lower limit on the visible energy. Events could be selected according to drastic cuts, which reject most of the "kinematical" effects due to ISR. Since $2E = E_{vis}/(1 + |\vec{\beta}|)$, where E is the energy of the incident electron and $|\vec{\beta}|$ is simply defined from the angles, one can determine the energy of the initially radiated photon from

$$kE_0 = 2E_0 - E_{vis}(1 + |\vec{\beta}|)$$

and make the relevant cut. Then, the remaining radiative corrections result mainly in some asymmetry on the ΔE errors, which become non- gaussian.

[4]the radiative factor is usually indicated with the symbol β and should not be confused with the velocity previously introduced

This effect can be taken into account. In an actual analysis, the selection cuts and fits are performed through various loops, with the measured energy being corrected at each step. In the case of H1, it has been observed that this procedure works remarkably well, with results which converge already at the second step.

In conclusion, we have outlined the main characteristics of a calibration method for the KLOE detector at DAΦNE , the ϕ-factory under completion in Frascati. Through the measurement of final state electron and photon produced through quasi-real Compton scattering, the method proposed will allow to check quantitatively the detector response in a continuous way in space and time. From a comparison with the case of the H1 detector at HERA, where the method has been successfully employed, we find that it is possible to achieve a one per mille accuracy on the energy calibration of KLOE (every 10 seconds of data taking). The complete calculation, with full Monte Carlo simulation, is under preparation and will be presented as a separate report.

The authors acknowledge the support of the European Economic Commission, HCMP Contract # CT920026.

References

[1] A.Courau and P.Kessler, Phys.Rev. D33 (1986) 2021.

[2] A.Courau and P.Kessler, Phys.Rev. D33 (1986) 2028; ib. D46, (1992) 117 and references therein.

[3] Delco collaboration, Phys.lett.B 177 (1986) 109.

[4] Cello collaboration, Phys. Lett. B168 (1986) 420.

[5] Venus collaboration, Phys. Lett. B213 (1988) 400.

[6] Aleph collab., Phys.lett.B 336 (1990) 501; Delphi collab., Zeit.fur.Phys C53 (1992) 41.

[7] H1 collaboration, Phys.lett.B 340 (1994) 205

[8] H1 collaboration, Z.Phys. C66 (1995) 529

S.Kermiche, Phd.thesis, University Paris-sud, LAL94-14(1994).

R. Maraček, 1997 Phd. Thesis, Institute for Experimental Physics, Kosiče (unpublished).

[9] KLOE Collaboration, "The KLOE Detector Technical Proposal", LNF-93/002, January 1993.

[10] G.Pancheri, Phys.Lett. B315 (1993) 477.

[11] M.Greco et al., Phys.lett.B318 (1993) 635.

[12] For a discussion of ISR at high energy e^+e^- collisions, see F.A. Berends and R. Kleiss, Nucl. Phys. B260 (1985) 32.

[13] E.Etim,G.Pancheri and B.Toushek, Nuovo Cimento B51 (1967) 276.

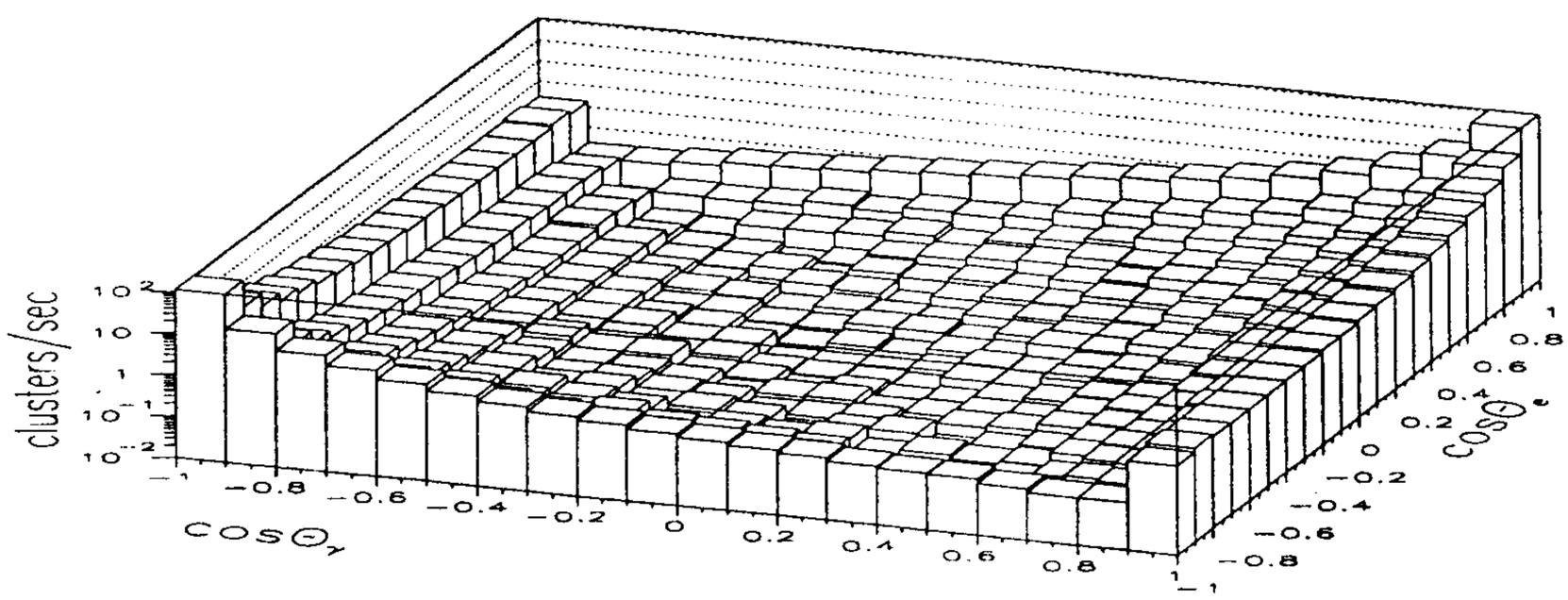

Figure 4: Angular configurations of the clusters for same conditions as in Fig.3.